Applied Physics B manuscript No.
(will be inserted by the editor)

A QCL-based metrological-grade source at 6 μm

D. D'Ambrosio[1,2], S. Borri[1,3], D. Calonico[2], C. Clivati[2], P. De Natale[1,3], M. De Pas[1,4], G. Insero[1,5], F. Levi[2], M. Verde[1], G. Santambrogio[1,2,3]

[1] Istituto Nazionale di Ottica, INO-CNR, & European Laboratory for Nonlinear Spectroscopy, LENS, Via Nello Carrara 1, 50019 Sesto Fiorentino, Italy

[2] Instituto Nazionale di Ricerca Metrologica, INRIM, Strada delle Cacce 91, 10135 Torino, Italy

[3] Istituto Nazionale di Fisica Nucleare, INFN, Sezione di Firenze, via G. Sansone 1, 50019 Sesto Fiorentino, FI, Italy

[4] Fritz-Haber-Institut der Max-Planck-Gesellschaft, Faradayweg 4–6, 14195 Berlin, Germany

[5] European Commission, Joint Research Centre (JRC), Karlsruhe, Germany

Received: date / Revised version: date

Abstract In view of high-precision molecular spectroscopy in the infrared, we realized a narrow-linewidth laser source at 5.8 μm traceable to the second in the International System of Units by mixing two near-infrared lasers in an orientation-patterned GaP crystal. The generated radiation is traceable to a Cs fountain through an optical fiber-delivered carrier; its estimated linewidth is 2.3 kHz at 1 s integration time. A quantum cascade laser emitting at the same wavelength is used to boost the power of the mid-IR radiation up to few tens of mW. Thanks to a phase-locking loop, about 70% of the quantum cascade laser output power is within the linewidth of the difference-frequency radiation. This apparatus is used for absolute molecular spectroscopy in a region, above 5 μm, where high precision traceability and reliable operation are still challenging. In this paper we provide the basic information to implement a powerful and metrological-grade source in the mid infrared for precision measurements.

1 Introduction

Molecular spectroscopy plays an important role in several fields and applications, including trace-gas sensing and precision measurements for fundamental research. The possibility to detect and quantify tiny quantities of a specific molecule in a gas sample has revolutionized not only environmental monitoring, but has also paved the way to the development of high-performance non-invasive diagnostic techniques for a number of different applications, including human health and safety [1,2], monitoring the state of conservation of food

[3], archaeological and climatological research [4,5], space applications [6].

From the perspective of fundamental physics, molecules are particularly appealing due to their rich internal structure and symmetry, and also for their strong intramolecular fields. They are used to investigate parity violation, to look for permanent electric dipole moments in fundamental particles, to test the CPT theorem, Lorentz symmetry, quantum electrodynamics, general relativity, spin-statistics theorem, to search for variations of fundamental constants, dark matter, dark energy and extra forces.[7,8] This new exciting class of measurements is expected to generate valuable information at fractional precisions better than 10^{-15}. Therefore, narrow-linewidth, powerful and stable laser sources are needed to achieve such levels of precision.

The mid-infrared (mid-IR) spectral region is characterized by intense, ro-vibrational molecular transitions with Hz-level natural line widths, and is the best candidate for spectroscopic measurements on low-density samples. This portion of the spectrum can be covered by quantum cascade lasers (QCLs), which have high spectral purity, large tuning capabilities, and mW-to-W output powers. These features are needed for detection of tiny amounts of molecules with reasonable signal-to-noise ratios (SNR); however, precision spectroscopy also requires highly coherent radiation traceable to primary frequency standards [9].

Various techniques for referencing QCL frequencies to the second in the International System of Units (SI) have been developed, the most widely investigated being mid-infrared optical combs generated by nonlinear frequency conversion, such as sum or difference frequency generation (SFG, DFG) [10,11]. An alternative approach is to generate mid-IR radiation by nonlinear processes involving near-IR lasers, traced to the SI via a commercial near-IR or visible comb. This latter approach has the advantage of an easier implementation, not requiring the nonlinear conversion of an entire, spectrally-wide optical comb, and relying on commercial, turn-key devices.

Although a number of implementations has been demonstrated [12], a significant improvement in terms of reliability, spectral coverage and performance is still necessary. Up to now, traceability for QCLs using near-IR combs has mostly been demonstrated at wavelengths below 5 μm. At longer wavelengths it is still challenging, mainly due to the difficulty in generating continuous-wavelength (cw) radiation with efficient nonlinear crystals. In this region, only a few papers have been published on this subject [11,13–17], demonstrating, however, impressive laser linewidths down to the 10-Hz level [11,17]. Another issue is related to the quality of the frequency standards used to reference mid-IR radiation [18]: until very recently, direct access to the best performing clocks was restricted to National Metrology Institutes (NMIs) and frequency dissemination was based on satellite techniques. Although such techniques allow ultimate uncertainties in the 10^{-16} region when operated at the highest level of complexity [19,20], most laboratories make use of commercial GPS-disciplined oscillators, whose instability is limited to 10^{-13} after one day average. Nowadays, the situation is rapidly chang-

ing, thanks to the possibility of delivering high-quality frequency reference signals up to continental distances using phase-stabilized optical fibers [21–27]. This technique was initially developed to enable clocks comparisons between NMIs; however, it has been adapted to meet the needs of non-NMI users by implementing specific technological solutions.

In this Letter, we describe the realization and frequency-noise characterization of a tunable source of coherent radiation around 5.8 μm wavelength. This source, having output powers in the few tens of mW range, is referred to the primary frequency standard at the Italian National Metrological Institute (INRIM) thanks to a 642-km long optical fiber link. This source has been used for high-precision spectroscopy on a metastable CO molecular beam, achieving 10^{-11} accuracy levels in measuring molecular frequencies [16] and transit-time limited resolution on the recorded absorption lines [28]. Here, we present a detailed description of the optical and electronic chain used to produce this radiation and to reference it to the primary frequency standard. The mid-IR radiation has an estimated linewidth of 2.3 kHz over 1 s timescale. Its long term stability reflects that of the H-maser at the base of the frequency chain, and is traceable to a primary frequency standard.

2 Experimental setup

2.1 Frequency reference

We transfer the stability and accuracy of the near-IR reference to the mid-IR using a commercial optical frequency comb (OFC) covering the 1-2 μm range (Menlo Systems GmbH, FC1500-100-WG). The comb is referenced to a 1542-nm ultrastable laser operated at INRIM (in Torino) and delivered to LENS (in Firenze) over the fiber link [22]. The optical reference at 1542 nm is a fiber laser whose frequency is kept at 194.399996 THz by a dual lock scheme: a fast Pound-Drever-Hall lock (bandwidth $>$ 60 kHz) to a high-finesse Fabry–Perot cavity [29] and a slow phase–lock (25 mHz bandwidth) to a hydrogen maser using an optical frequency comb, to correct for the cavity long-term instability. The stability of this laser is $3{\cdot}10^{-15}$ at 1 s. A periodic comparison of the hydrogen maser with a cryogenic Cs fountain primary frequency standard [30] ensures absolute traceability of the 1542-nm laser frequency.

This optical signal is sent to the laboratory at LENS via a 642-km-long fiber link, where 9 bidirectional erbium-doped fiber amplifiers have been installed to partly compensate for the 190-dB optical losses [22]. The optical phase is stabilized using the Doppler noise cancellation scheme [31]. At LENS, a diode laser (regeneration laser, RIO PLANEX Laser) is phase-locked to the incoming radiation on a bandwidth of 100 kHz, boosting the optical power at a suitable level for referencing the local frequency comb [32]. A complete metrological characterization of the fiber-delivered frequency signal can be found in [32]. While GPS dissemination limits the typical fractional frequency uncertainty to 10^{-13} on a day average [33], frequency dissemination by fiber link allows to achieve a short-term Allan deviation of 1×10^{-14} at 1 s and

an ultimate accuracy on the frequency transfer of 5×10^{-19} at 1000 s integration time [32].

2.2 Overview of the locking chain

An overview of the experimental setup at LENS is shown in Fig. 1. The frequency difference of two lasers, one at 1064 nm (pump, InnoLight GmbH, Mephisto MOPA 55W) and the other at 1301 nm (signal, Toptica Photonics AG, DL PRO), is kept fixed by locking the pump laser to the OFC and the signal laser to the pump via the so-called virtual beat-note scheme. Radiation at the difference frequency (DF), i.e. around 5.8 μm, is generated in a 24.6-mm long OP-GaP crystal [34]. The crystal has a 400 μm-thick unpatterned GaP substrate, over which the OP layer extends for another 400 μm thickness, with a 50% duty cycle periodic domain reversal (the grating period is 24 μm). The sample is housed in a massive copper-block oven whose temperature is regulated by a P-I servo-controller to optimize phase-matching. After the crystal, the idler beam is separated from the others using a coated Ge window. With $\sim$10 W of pump and $\sim$40 mW of signal, up to 65 μW of idler radiation are generated, limited by thermal dephasing effects in the crystal. This radiation is used to lock the frequency of a room-temperature DFB-QCL (Alpes Lasers) that delivers up to 35 mW of mid-IR light. The beat note is generated on a thermo-electric cooled HgCdTe photodiode with a bandwidth of tens of MHz. Such a signal is used to feed a phase-locked loop (PLL3 in Fig. 1) that stabilizes the QCL by modulating its current with a bandwidth of 300 kHz. Once locked, the frequency of the QCL can be finely tuned with respect to the DFG frequency by changing the frequency reference of PLL3. This allows us to tune the QCL vs DFG frequency over 80MHz, limited by the bandwidth of the HgCdTe detector.

2.3 Detailed description of the setup

The repetition rate frequency f_{rep} of the OFC is phase-locked to the 1542-nm light using an intra-cavity electro-optic modulator. The achieved locking bandwidth is approximately 300 kHz, and the lock frequency is properly chosen so that the repetition rate is exactly 100 MHz when the incoming radiation is at the nominal frequency value. The carrier-envelope offset frequency f_0 is stabilized at a value of 20 MHz to a radio-frequency (RF) standard (GPS-disciplined Rubidium oscillator). The phase noise of the optical comb is limited by the optical reference that is delivered over the fiber link. In particular, in the acoustic region the fiber-induced phase noise is not completely suppressed due to the limited bandwidth of the Doppler noise cancellation loop. In fact, this is inversely proportional to the round-trip time of the light in the fiber [31] and it amounts to about 40 Hz in our link [22]. To overcome this limitation, we exploit the good short-term stability of our pump laser, as explained in Sec.2.4.

The power for each comb tooth is of the order of 100 nW, on average. We split the comb output into two arms to measure the beat notes with the pump and the signal lasers. For this, we use a dichroic mirror that separates the two spectral regions with over 95% efficiency. For a good SNR on the detector, laser beam collimation is important. To minimize

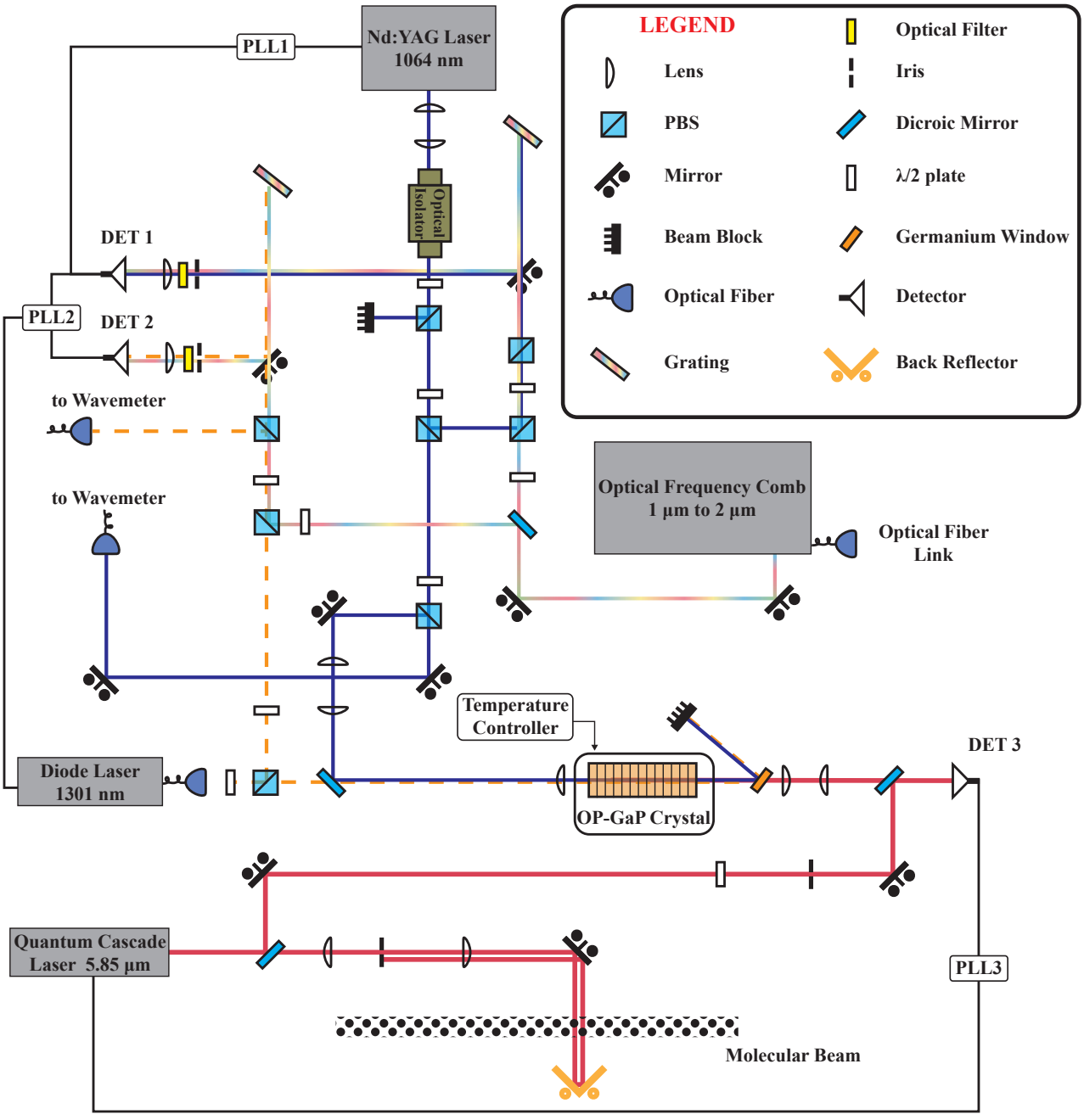

Fig. 1 Scheme of the optical setup. The optical fiber link from INRIM is used to lock an optical comb. Two lasers, at 1064 nm and at 1301 nm, are phase-locked to the comb through the so-called virtual beat-note scheme. The two lasers are mixed in a OP-GaP crystal to produce their difference in frequency. Finally, a QCL is phase-locked to this mid-IR light and can be used, for instance, for molecular spectroscopy.

power losses, we use a telescope on the comb beam before the dichroic mirror, although the refraction index difference at the two frequencies yields an imperfect collimation. We isolate the teeth needed for each beat note using two gratings mounted in Littrow configuration, followed by apertures to further improve selectivity.

The PLL electronics we developed requires the SNR of the input RF to be better than 30 dB in 100 kHz. Tweeking of the OFC amplifier yields SNR of the order of 25–30 dB. By measuring each beat note with two InGaAs photodiodes used in differential configuration, we improved the SNR by about 10 dB, reaching a best-case condition of 40 dB SNR in 100 kHz bandwidth.

The diode laser is phase-locked to the pump to stabilize the difference frequency $\nu_{\mathrm{DF}} = \nu_{\mathrm{pump}} - \nu_{\mathrm{signal}}$, where ν_{pump} and ν_{signal} are the absolute frequencies of the two lasers. Here and in the following we use ν for optical frequencies and f for radiofrequencies. The frequency difference between the two lasers is bridged using the OFC as transfer oscillator, with the so-called *virtual beat note* scheme [35,36]. To implement the virtual beat note, the offset frequency f_0 is mixed with each beat note $f_{\mathrm{b:pump}}$ and $f_{\mathrm{b:signal}}$ using analog mixers, to produce $\overline{f}_{\mathrm{b:pump}} = f_{\mathrm{b:pump}} + f_0$ and $\overline{f}_{\mathrm{b:signal}} = f_{\mathrm{b:signal}} + f_0$. Thus, the absolute frequencies of the two lasers can be written as $\nu_{\mathrm{pump}} = n_{\mathrm{pump}} f_{\mathrm{rep}} + f_0 + f_{\mathrm{b:pump}} = n_{\mathrm{pump}} f_{\mathrm{rep}} + \overline{f}_{\mathrm{b:pump}}$ and $\nu_{\mathrm{signal}} = n_{\mathrm{signal}} f_{\mathrm{rep}} + f_0 + f_{\mathrm{b:signal}} = n_{\mathrm{signal}} f_{\mathrm{rep}} + \overline{f}_{\mathrm{b:signal}}$, where $n_{\mathrm{pump}} = 2816364$ and $n_{\mathrm{signal}} = 2302371$ are the numbers of the comb's teeth to which the two lasers are beaten, and $f_{\mathrm{b:pump}}$ and $f_{\mathrm{b:signal}}$ have to be taken with their sign (not necessarily positive). In our case, for electronics and filtering needs, $f_{\mathrm{b:pump}}$ has to be considered as negative (-130 MHz, beating with the second comb tooth on the right) while $f_{\mathrm{b:signal}}$ is positive (70 MHz, beating with the tooth on the left). The value of n_{pump} and n_{signal} can be easily calculated thanks to a preliminary measurement of the pump and signal frequency with a commercial wavelength meter (Bristol 621A-NIR, 60 MHz accuracy). The signal $(n_{\mathrm{signal}}/n_{\mathrm{pump}})\overline{f}_{\mathrm{b:pump}} - \overline{f}_{\mathrm{b:signal}}$ is generated with a 32-bit Direct Digital Synthesizer (DDS) and a mixer, and is used as the error signal for the phase–lock loop (PLL) of the diode laser with a bandwidth of about 100 kHz. An overview of the electronics used for the virtual beat-note scheme is shown in Figure 2.

2.4 The virtual beat-note method

This procedure is thoroughly described in Ref. [35] and is a well-established method in many laboratories. For a more intuitive understanding, we can first think of a simplified case in which the DF of two lasers is locked using a comb whose f_{rep} is perfectly fixed. The free parameters in this case are the frequencies of the two lasers, ν_{pump} and ν_{signal}, and the comb's offset f_0. Since the DF is assumed to be too large to be counted directly, each laser is beaten against the closest tooth of the OFC, yielding $f_{\mathrm{b:pump}} = \nu_{\mathrm{pump}} - (n_{\mathrm{pump}} f_{\mathrm{rep}} + f_0)$ and $f_{\mathrm{b:signal}} = \nu_{\mathrm{signal}} - (n_{\mathrm{signal}} f_{\mathrm{rep}} + f_0)$, and a PLL keeps the difference

$$f_{\mathrm{b:pump}} - f_{\mathrm{b:signal}} = (\nu_{\mathrm{pump}} - \nu_{\mathrm{signal}}) - f_{\mathrm{rep}}(n_{\mathrm{pump}} - n_{\mathrm{signal}}) \quad (1)$$

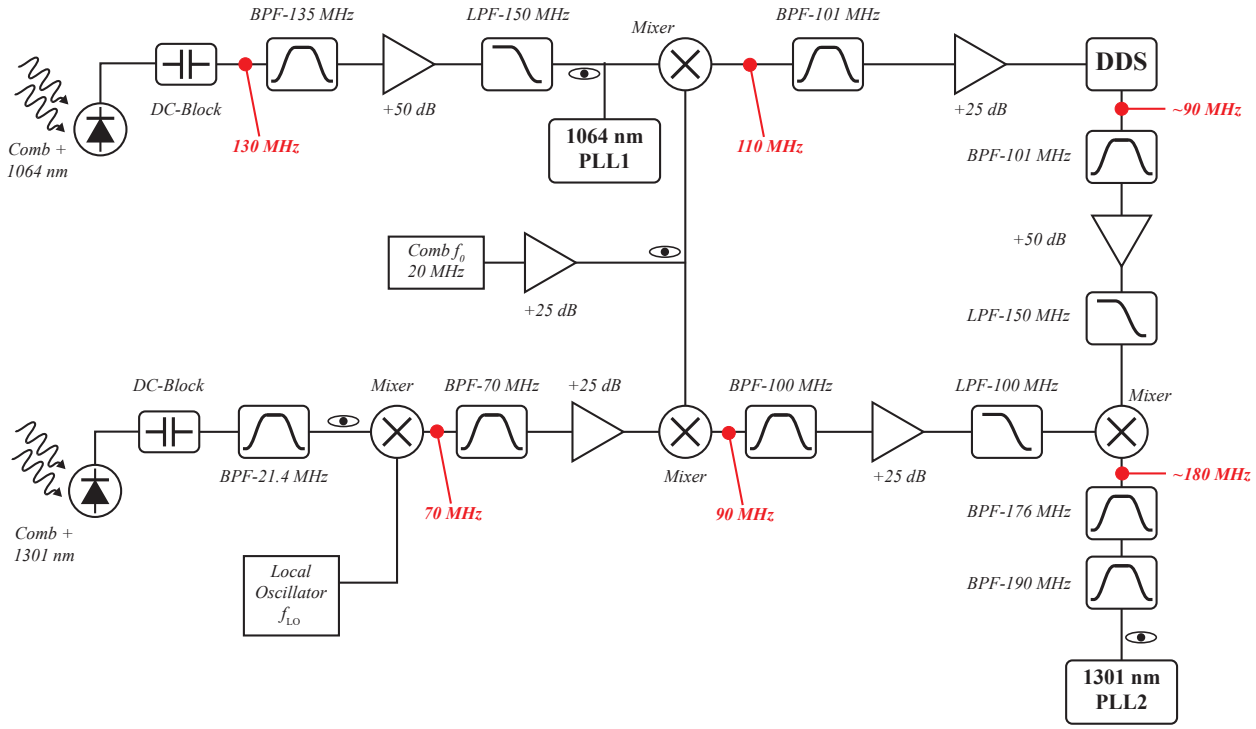

Fig. 2 Scheme of the electronics used to implement the virtual beat-note locking scheme. Band-pass and low-pass filters are indicated as BPF and LPF, followed by the central frequency and the cut frequency, respectively. In locking conditions, the local oscillator f_{LO} acts on the signal laser and allows to tune its frequency, thus leading to additional tuning of the QCL. The absolute value of the main frequencies in various position is indicated in red. As indicated by the theory, f_0 is always added to the beat note $f_{\mathrm{b:pump}}$ and $f_{\mathrm{b:signal}}$, that, in our case, are negative and positive respectively.

constant by acting on the frequency of either laser, say the signal. We note that the value $f_{\mathrm{b:pump}} - f_{\mathrm{b:signal}}$ is all the PLL needs, whereas knowledge of which of the free parameters is drifting is irrelevant. Thus, the pump could in principle run unlocked but this is unpractical, since the photodiodes and the filters have a limited bandwidth. So, we lock the pump frequency to the comb, and we use the beat note $\overline{f}_{\mathrm{b:pump}} = f_{\mathrm{b:pump}} + f_0$ instead of $f_{\mathrm{b:pump}}$ to avoid unnecessary action on the pump's driver to follow instabilities in f_0. Once $\overline{f}_{\mathrm{b:pump}}$ has been generated with a mixer, the same can be done for the signal and the DF for the PLL is thus generated as $\overline{f}_{\mathrm{b:pump}} - \overline{f}_{\mathrm{b:signal}}$, which is identical to equation 1.

If a real OFC is used instead, where the stability of f_{rep} is finite, one immediately sees from equation 1 that the difference of the beat notes is not a good signal for the PLL because the term $f_{\mathrm{rep}}(n_{\mathrm{pump}} - n_{\mathrm{signal}})$ is not constant anymore. A conceptual difficulty arises by the fact that a variation of $\overline{f}_{\mathrm{b:pump}} - \overline{f}_{\mathrm{b:signal}}$ could either be due to a drift in the pump's or signal's frequency, or to a drift of f_{rep}. The appropriate correction to apply to the signal's frequency to keep DF constant would be a shift of equal size in the first case, but a

shift scaled by $n_{\text{signal}}/n_{\text{pump}}$ in the latter case, because of the stretchable-ribbon-like behavior of OFCs. A simple solution is available if the pump has a good short-term stability and can thus be loosely locked to a comb's tooth. Then, the PLL for the signal (PLL 2 in Fig. 1) can be closed on

$$\frac{n_{\text{signal}}}{n_{\text{pump}}}\overline{f}_{\text{b:pump}} - \overline{f}_{\text{b:signal}} \quad (2)$$

with a much tighter lock, i.e with a wider bandwidth.

Once all the lasers are properly locked, eq.2 is kept to a constant value (180 MHz in our case). According to the DDS technique, the difference frequency is given by

$$\nu_{\text{DF}} = (1 - \frac{n_{\text{signal}}}{n_{\text{pump}}})\ \nu_{\text{pump}} + (\frac{n_{\text{signal}}}{n_{\text{pump}}}\overline{f}_{\text{b:pump}} - \overline{f}_{\text{b:signal}}) \quad (3)$$

The phase noise of the DF, $S_{\phi,\text{DF}}$, can be derived from eq.3. The last term in the equation is kept constant by the PLL, and its contribution to the DF noise comes from the phase noise of the locking electronics. This contribution can be easily measured and it resulted to be much smaller than the phase noise of the pump laser. The phase noise $S_{\phi,\text{DF}}$ is thus expected to depend on the pump phase noise only, $S_{\phi,\text{pump}}$, according to

$$S_{\phi,\text{DF}} = (1 - \frac{n_{\text{signal}}}{n_{\text{pump}}})^2\ S_{\phi,\text{pump}} \quad (4)$$

with a rescaling factor $(1 - \frac{n_{\text{signal}}}{n_{\text{pump}}})^2$ which, in our case, is $\simeq 0.033$.

3 Characterization of the mid-IR radiation

In order to give a full characterization of the frequency stability and phase noise of our lasers, including the mid-IR DF radiation, we started from independent measurements of the phase noise of the reference radiation at 1542 nm and from a noise analysis of the near-IR lasers. The free-running PNPSD of both the pump and signal lasers, beating with the relative comb teeth, is shown in figure 3. It was retrieved from the spectra of the feedback signals exiting the PLLs (PLL1 and PLL2) and going to the laser drivers. The expected noise of the related comb teeth, also shown in the figure, was calculated from the link noise, derived from independent measurements [32], rescaled to the respective spectral regions. We can see that phase noise on $f_{\text{b:pump}}$ reproduces the comb noise at 1064 nm at frequencies higher than 50 Hz, which means that the comb noise dominates in this region. It appears then straightforward to implement a loose locking of

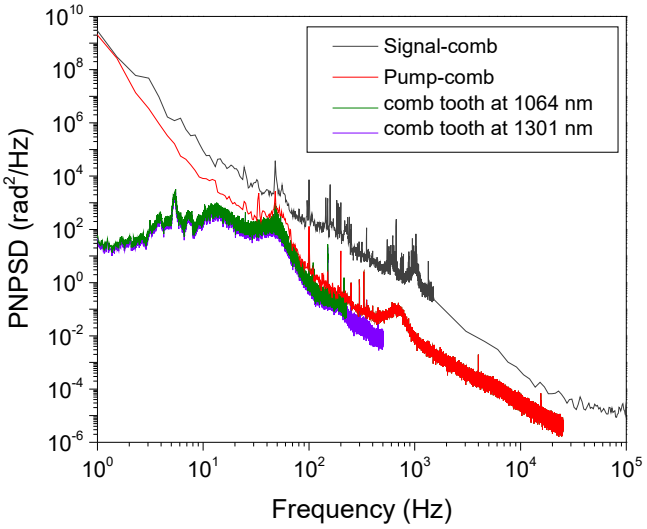

Fig. 3 Estimated and measured phase noise power spectral densities (PNPSD). The phase noise of the comb tooth n_{pump} and n_{signal} are obtained from independent measurement of the PNPSD of the reference radiation at 1542.14 nm. The phase noise of the free-running pump and signal beating with the comb (red and black curves, respectively) are obtained calculating the PNPSD from the PLL output signal (PLL1 and PLL2, respectively) sent to the different laser drivers for locking.

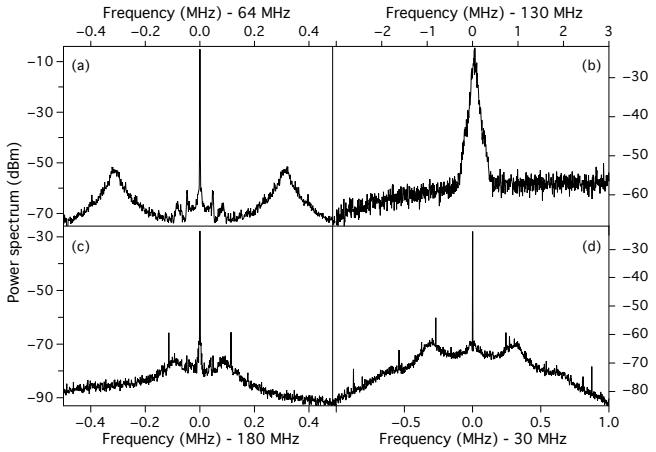

Fig. 4 Beat notes of the different phase-lock loops acquired by means of a spectrum analyzer. (a): beat note between the comb and the reference laser at 1542 nm. Beat note between comb and pump (b) and virtual beat note between pump and signal (c). (d): beat note between the generated DFG and the QCL. All spectra are acquired with 10 Hz resolution bandwidth, except the data shown in (b) for which the resolution bandwidth is 300 Hz.

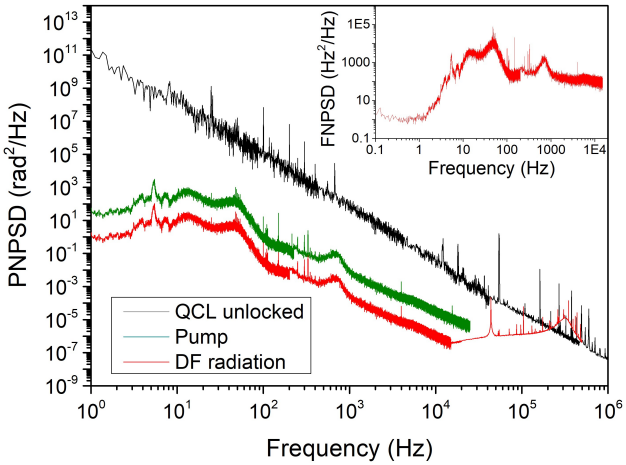

Fig. 5 Phase noise of the free-running QCL (black), of the pump laser (green) and of the DF radiation (red). The residual phase noise of the pump laser, in locking conditions, is estimated to be limited by the comb noise within the PLL bandwidth (green trace of Fig.3). Data from Ref.[16]. In the inset, the frequency-noise PSD of the DF radiation is shown.

the pump laser to the comb, limiting the locking bandwidth at a frequency around 50 Hz, using the pump itself as reference oscillator at short timescales.

In figure 4 some typical recordings of the beat notes between different lasers are shown. The plot (a) shows the beat note between the comb and the regenerated reference light at 1542 nm. A PLL stabilizes the beat-note frequency at 64 MHz to maintain the repetition rate of our comb at 100 MHz. Panel (b) shows the beat note between the comb tooth and the 1064 nm laser. In this case the beat note is stabilized at 130 MHz and it is broad because of the low locking bandwidth of about 500 Hz. On graphs (c) and (d) the virtual beat note between the 1064 nm and the 1300 nm laser and the beat note between the QCL and the DFG radiation are shown. The smoothed sidebands around the carrier correspond to the servo bumps. From these we infer a locking bandwidth of 300 kHz in (a) and (d) and 100 kHz in (c). In (b) the servo bumps are not visible because of the limited resolution bandwidth and the loose locking of the pump laser to the comb.

When we lock a laser in phase to a reference, we want that as much power as possible is emitted into the reference mode. This can be easily measured by integrating the beat-note spectrum of the two lasers and comparing the total area under the beat note with that underlying the peak only. From a numerical integration of the different portions of the spectrum of the beat note between QCL and DF radiation shown in Fig. 4d, we estimate that about 70% of the QCL power is within the bandwidth of the DF mode. This value, mainly limited by the bandwidth of the locking loop, is comparable

with similar results obtained with locked QCLs in previous works with different electronic locking schemes [37,18]. In this condition, we expect that the QCL absolute frequency is determined with the same accuracy as the DF radiation, and that its linewidth does not deviate significantly from that of the DF radiation.

A direct phase noise measurement of the generated mid-IR radiation could be obtained by comparing two identical systems. However, the duplication of the entire setup is a too big effort, at least for cost reasons. Alternatively, one could exploit a sufficiently narrow absorption line as a frequency-to-amplitude discriminator. In our case, this could not be realized, because all available absorption lines at this wavelengh are not sharp enough to overcome the limitation of the intrinsic electrical noise of the mid-IR detectors [28]. Nonetheless, according to Eq. 4, the DF phase noise can be estimated from the PNPSD of the pump. Fig. 5 shows the pump PNPSD (green trace) and the expected phase noise of the DF radiation (red trace). For frequencies above 15 kHz the DF noise is dominated by the background due to electronic noise (thinner red trace). In the inset, the DF radiation frequency noise PSD is also shown. From a numerical integration of the frequency noise PSD, according to [38], we calculate a linewidth of 2.3 kHz (FWHM over 1 s timescale) for the DF radiation. This is expected to match the linewidth of the QCL when locked to the DF light. In the figure, the phase noise of the free-running QCL is also shown for comparison (black trace), recorded by using the mode of an optical resonator as frequency-to-amplitude converter and corresponding to a linewidth of about 1 MHz (HWHM) [28].

It is worth noting that the present limitation to the QCL linewidth comes from the short-term stability of the optical 1542-nm reference and of the pump laser. This limitation may be overcome with minimum changes in our apparatus by adopting an ultra-narrow telecom laser for local regeneration of the fiber-link signal. In this case, the comb may be tightly stabilized to the reference signal and the pump and signal lasers may be, in turn, tightly locked to the comb, thus leading to narrower idler (and QCL) radiation.

In the former analysis, we have assumed that the phase-lock loops are driven by a noiseless local oscillator. Actually, all the PLLs and local oscillators used in the locking chain are referenced to a local GPS-disciplined Rubidium-based reference that has a relative stability of $\simeq 1 \cdot 10^{-12}$. We calculate a contribution to the final stability of the mid-IR radiation of few parts in 10^{-18}, which is negligible with respect to the stability of the optical link.

4 Conclusion

In this paper we have described a novel hybrid QCL/DFG source emitting around 6 μm wavelength. By exploiting referencing to a telecom carrier distributed by the Italian fiber link, that is traceable to the primary frequency standard, we obtain tunable mid-IR radiation with $\sim$10-mW power and absolute traceability. Moreover, by using the OFC as a transfer oscillator for the DFG pump and signal, we can concentrate

more than 70% of the power within the reference laser bandwidth, obtaining a 2.3 kHz linewidth (at 1 s).

Finally, it is worth remarking that our scheme can be applied in other spectral regions, with appropriate sources. We expect that our method will be useful for the most challenging experiments making use of molecular spectroscopy, e.g. for laser cooling of molecules, a research area developing at very fast pace and requiring mid and far IR laser sources for manipulating their rovibrational degrees of freedom.

Funding

This work was partially funded by INFN under the SUPREMO project and Ente Cassa di Risparmio di Firenze under the COSMO project.

Acknowledgments

The authors gratefully acknowledge dr. Samuel Meek for designing and providing the balanced photodiodes.

References

1. S. Svanberg, "Laser spectroscopy for medical applications," in "Laser Spectroscopy for Sensing," , M. Baudelet, ed. (Woodhead Publishing, 2014), pp. 421 – 460.
2. I. Bayrakli, "Breath analysis using external cavity diode lasers: a review," J. Biomed. Opt. **22**, 040901 (2017).
3. S. Svanberg, G. Zhao, H. Zhang, J. Huang, M. Lian, T. Li, S. Zhu, Y. Li, Z. Duan, H. Lin, and K. Svanberg, "Laser spectroscopy applied to environmental, ecological, food safety, and biomedical research," Opt. Express **24**, A515 (2016).
4. I. Galli, S. Bartalini, R. Ballerini, M. Barucci, P. Cancio, M. D. Pas, G. Giusfredi, D. Mazzotti, N. Akikusa, and P. D. Natale, "Spectroscopic detection of radiocarbon dioxide at parts-per-quadrillion sensitivity," Optica **3**, 385 (2016).
5. A. J. Fleisher, D. A. Long, Q. Liu, L. Gameson, and J. T. Hodges, "Optical measurement of radiocarbon below unity fraction modern by linear absorption spectroscopy," J. Phys. Chem. Lett. **8**, 4550 (2017).
6. T. Steinmetz, T. Wilken, C. Araujo-Hauck, R. Holzwarth, T. W. Hänsch, L. Pasquini, A. Manescau, S. D'Odorico, M. T. Murphy, T. Kentischer, W. Schmidt, and T. Udem, "Laser frequency combs for astronomical observations," Science **321**, 1335 (2008).
7. D. DeMille, J. M. Doyle, and A. O. Sushkov, "Probing the frontiers of particle physics with tabletop-scale experiments," Science **357**, 990 (2017).
8. M. Safronova, D. Budker, D. DeMille, D. F. J. Kimball, A. Derevianko, and C. W. Clark, "Search for new physics with atoms and molecules," Rev. Mod. Phys. **90**, 025008 (2018).
9. S. Borri and G. Santambrogio, "Laser spectroscopy of cold molecules," Advances in Physics: X **1**, 368 (2016).
10. A. Schliesser, N. Picqué, and T. W. Hänsch, "Mid-infrared frequency combs," Nature Phot. **6**, 440 (2012).
11. B. Argence, B. Chanteau, O. Lopez, D. Nicolodi, M. Abgrall, C. Chardonnet, C. Daussy, B. Darquié, Y. L. Coq, and A. Amy-Klein, "Quantum cascade laser frequency stabilization at the sub-Hz level," Nature Phot. **9**, 456 (2015).
12. U. Bressel, I. Ernsting, and S. Schiller, "5 μm laser source for frequency metrology based on difference frequency generation," Opt. Lett. **37**, 918 (2012).
13. M. G. Hansen, I. Ernsting, S. V. Vasilyev, A. Grisard, E. Lallier, B. Gérard, and S. Schiller, "Robust, frequency-stable

and accurate mid-IR laser spectrometer based on frequency comb metrology of quantum cascade lasers up-converted in orientation-patterned GaAs," Opt. Express **21**, 27043 (2013).

14. A. Gambetta, M. Cassinerio, N. Coluccelli, E. Fasci, A. Castrillo, L. Gianfrani, D. Gatti, M. Marangoni, P. Laporta, and G. Galzerano, "Direct phase-locking of a 8.6-μm quantum cascade laser to a mid-IR optical frequency comb: application to precision spectroscopy of N_2O," Opt. Lett. **40**, 304 (2015).
15. M. Lamperti, B. AlSaif, D. Gatti, M. Fermann, P. Laporta, A. Farooq, and M. Marangoni, "Absolute spectroscopy near 7.8 μm with a comb-locked extended-cavity quantum-cascade-laser," Sci. Reports **8**, 1292 (2018).
16. G. Insero, S. Borri, D. Calonico, P. C. Pastor, C. Clivati, D. D'Ambrosio, P. D. Natale, M. Inguscio, F. Levi, and G. Santambrogio, "Measuring molecular frequencies in the 1–10 μm range at 11-digits accuracy," Sci. Reports **7**, 12780 (2017).
17. M. G. Hansen, E. Magoulakis, Q.-F. Chen, I. Ernsting, and S. Schiller, "Quantum cascade laser-based mid-IR frequency metrology system with ultra-narrow linewidth and 1×10^{-13}-level frequency instability," Opt. Lett. **40**, 2289 (2015).
18. I. Galli, M. S. de Cumis, F. Cappelli, S. Bartalini, D. Mazzotti, S. Borri, A. Montori, N. Akikusa, M. Yamanishi, G. Giusfredi, P. Cancio, and P. D. Natale, "Comb-assisted subkilohertz linewidth quantum cascade laser for high-precision mid-infrared spectroscopy," Appl. Phys. Lett. **102**, 121117 (2013).
19. M. Fujieda, D. Piester, T. Gotoh, J. Becker, M. Aida, and A. Bauch, "Carrier-phase two-way satellite frequency transfer over a very long baseline," Metrologia **51**, 253 (2014).
20. G. Petit, A. Kanj, S. Loyer, J. Delporte, F. Mercier, and F. Perosanz, "1x10^{-16} frequency transfer by GPS PPP with integer ambiguity resolution," Metrologia **52**, 301 (2015).
21. C. Lisdat, G. Grosche, N. Quintin, C. Shi, S. Raupach, C. Grebing, D. Nicolodi, F. Stefani, A. Al-Masoudi, S. Dörscher, S. Häfner, J.-L. Robyr, N. Chiodo, S. Bilicki, E. Bookjans, A. Koczwara, S. Koke, A. Kuhl, F. Wiotte, and F. Meynadier, "A clock network for geodesy and fundamental science," Nature Comm. **7**, 12443 (2016).
22. D. Calonico, E. K. Bertacco, C. E. Calosso, C. Clivati, G. A. Costanzo, M. Frittelli, A. Godone, A. Mura, N. Poli, D. V. Sutyrin, G. Tino, M. E. Zucco, and F. Levi, "High-accuracy coherent optical frequency transfer over a doubled 642-km fiber link," Appl. Phys. B **117**, 979 (2014).
23. L. Sliwczynski, P. Krehlik, A. Czubla, L. Buczek, and M. Lipinski, "Dissemination of time and RF frequency via a stabilized fibre optic link over a distance of 420 km," Metrologia **50**, 133 (2013).
24. S. C. Ebenhag, P. O. Hedekvist, P. Jarlemark, R. Emardson, K. Jaldehag, C. Rieck, and P. Lothberg, "Measurements and error sources in time transfer using asynchronous fiber network," IEEE Trans. Instrum Meas. **59**, 1918 (2010).
25. F. L. Hong, M. Musha, M. Takamoto, H. Inaba, S. Yanagimachi, A. Takamizawa, K. Watabe, T. Ikegami, M. Imae, Y. Fujii, M. Amemiya, K. Nakagawa, K. Ueda, and H. Katori, "Measuring the frequency of a Sr optical lattice clock using a 120 km coherent optical transfer," Opt. Lett. **34**, 692 (2009).
26. B. Wang, C. Gao, W. Chen, J. Miao, X. Zhu, Y. Bai, J. Zhang, Y. Feng, T. Li, and L. Wang, "Precise and continuous time and frequency synchronization at the $5\times$1E-19 accuracy level," Sci. Reports **2**, 556 (2012).
27. G. Marra, R. Slavik, H. S. Margolis, S. N. Lea, P. Petropoulos, D. J. Richardson, and P. Gill, "High resolution microwave frequency transfer over a 86 km long optical fibre network using

an optical frequency comb," Opt. Lett. **36**, 511 (2011).

28. D. D'Ambrosio, S. Borri, M. Verde, A. Borgognoni, G. Insero, P. D. Natale, and G. Santambrogio, "Approaching the transit time limit for high-precision spectroscopy on metastable CO around 6 μm," Phys. Chem. Chem. Phys. **21**, 24506 (2019).
29. C. Clivati, A. Mura, D. Calonico, F. Levi, G. A. Costanzo, C. E. Calosso, and A. Godone, "Planar-waveguide external cavity laser stabilization for an optical link with 10^{-19} frequency stability," IEEE Trans. Ultrason. Ferroelectr. Freq. Contr. **58**, 2582 (2011).
30. F. Levi, D. Calonico, C. E. Calosso, A. Godone, S. Micalizio, and G. A. Costanzo, "Accuracy evaluation of ITCsF2: a nitrogen cooled caesium fountain," Metrologia **51**, 270 (2014).
31. P. A. Williams, W. C. Swann, and N. R. Newbury, "High-stability transfer of an optical frequency over long fiber-optic links," J. Opt. Soc. Am. B **25**, 1284 (2008).
32. C. Clivati, G. Cappellini, L. F. Livi, F. Poggiali, M. S. de Cumis, M. Mancini, G. Pagano, M. Frittelli, A. Mura, G. A. Costanzo, F. Levi, D. Calonico, L. Fallani, J. Catani, and M. Inguscio, "Measuring absolute frequencies beyond the GPS limit via long-haul optical frequency dissemination," Opt. Express **24**, 11865 (2016).
33. M. A. Lombardi, "The use of GPS disciplined oscillators as primary frequency standards for calibration and metrology laboratories," NCSLI Measure J. Meas. Sci. **3**, 56 (2008).
34. G. Insero, C. Clivati, D. D'Ambrosio, P. D. Natale, G. Santambrogio, P. Schunemann, J.-J. Zondy, and S. Borri, "Difference frequency generation in the mid-infrared with orientation-patterned gallium phosphide crystals," Opt. Lett. **41**, 5114 (2016).
35. H. Telle, B. Lipphardt, and J. Stenger, "Kerr-lens, mode-locked lasers as transfer oscillators for optical frequency measurements," Appl. Phys. B **74**, 1 (2002).
36. I. Galli, S. Bartalini, P. Cancio, G. Giusfredi, D. Mazzotti, and P. D. Natale, "Ultra-stable, widely tunable and absolutely linked mid-IR coherent source," Opt. Express **17**, 9582 (2009).
37. F. Cappelli, I. Galli, S. Borri, G. Giusfredi, P. Cancio, D. Mazzotti, A. Montori, N. Akikusa, M. Yamanishi, S. Bartalini, and P. D. Natale, "Subkilohertz linewidth room-temperature mid-infrared quantum cascade laser using a molecular sub-Doppler reference," Opt. Lett. **37**, 4811 (2012).
38. D. S. Elliott, R. Roy, and S. Smith, "Extracavity laser band-shape and bandwidth modification," Phys. Rev. A **26**, 12 (1982).